AJNR

Inflammatory diseases of the brain in childhood.

C R Fitz

AJNR Am J Neuroradiol 1992, 13 (2) 551-567
http://www.ajnr.org/content/13/2/551.citation

This information is current as
of April 17, 2024.

Inflammatory Diseases of the Brain in Childhood

Charles R. Fitz[1]

From the Children's National Medical Center, Washington, DC

Pediatric inflammatory disease may resemble adult disease or show remarkable, unique characteristics. This paper summarizes the current imaging of pediatric diseases with emphasis on those that are the most different from adult illnesses.

Congenital Infections

Most intrauterine infections are acquired through the placenta, although transvaginal bacterial infections may also occur. The TORCH eponym remains a good reminder for these entities, identifying toxoplasmosis, others, rubella, cytomegalic virus, and herpes simplex. A second H for HIV or perhaps the words A (AIDS) TORCH should now be used, as AIDS becomes the most common maternally transmitted infection.

Toxoplasmosis

This infection is passed to humans from cats, since the oocyst of the *Toxoplasma gondii* parasite is excreted in cat feces. The incidence of seropositive adult human females is about 90% in France and in some parts of the United States (1). Congenital infection occurs only when the mother becomes infected during pregnancy. Toxoplasmosis is said to affect 3% of pregnancies in France (2), and between 1 in 1,000 to 1 in 8,000 pregnancies in the Unites States (1). The most complete recent radiologic report of the condition is Diebler et al's review of 31 infants (2). They found that the frequency of congenital involvement increases with each trimester, being 17%, 25%, and 65%. However, infection severity decreases in each trimester. The true frequency of early cases may have been underestimated in their study, because spontaneous abortions were not included in the retrospective analysis.

Intracranial calcification is the most notable radiologic sign. Basal ganglial, periventricular, and peripheral locations are all common (Fig. 1). Large basal ganglial calcifications are related to early infection, as is hydrocephalus. The hydrocephalus is invariably secondary to aqueductal stenosis (2), and often has a characteristically marked expansion of the atria and occipital horns (Fig. 2), probably partly due to associated tissue loss. This is associated with increased periventricular calcification in the author's experience. Microcephaly is common, and encephalomalacia is seen occasionally (2). Hydrencephaly has also been reported (3).

Because calcifications are common and fairly characteristic, computed tomography (CT) is preferable to magnetic resonance (MR) imaging for diagnosis. Clinically, infants infected with *T. gondii* most commonly show chorioretinitis, seizures, and developmental delay.

Cytomegalovirus

Cytomegalic virus (CMV) is a herpes virus that infects nearly every person at some time in his life. Congenital infection occurs when maternal infection or reactivation of infection happens during pregnancy (4). The incidence of infection is considerably higher in lower socioeconomic than middle-class women, with a seroconversion rate of 6% per year versus 2% per year in the two groups (4). As with toxoplasmosis, earlier maternal infection results in a more severe infant infection (5). Up to 2% of newborns are said to be positive for the virus (6). At the author's hospital,

[1] Address reprint requests to Dr Fitz at the Department of Radiology, Children's Hospital of Pittsburgh, 3705 5th Ave, Pittsburgh, PA 15213.

Index terms: Brain, infection; Encephalitis; Pediatric neuroradiology; Acquired immunodeficiency syndrome (AIDS)

AJNR 13:551–567, Mar/Apr 1992 0195-6108/92/1302-0551
© American Society of Neuroradiology

Fig. 1. Toxoplasmosis in a 1-month-old infant; noncontrast CT. There is extensive basal ganglia calcification plus peripheral calcification primarily in the subcortical white matter. Diffuse atrophy and ventricular enlargement are present. (Courtesy of Dr Carl Geyer, Walter Reed Army Medical Center, Washington, DC.)

Fig. 2. Toxoplasmosis with calcification and hydrocephalus; noncontrast CT in a 3½-week-old infant. There is severe hydrocephalus, periventricular and peripheral calcification, and intraventricular calcification, probably on inflammatory septations.

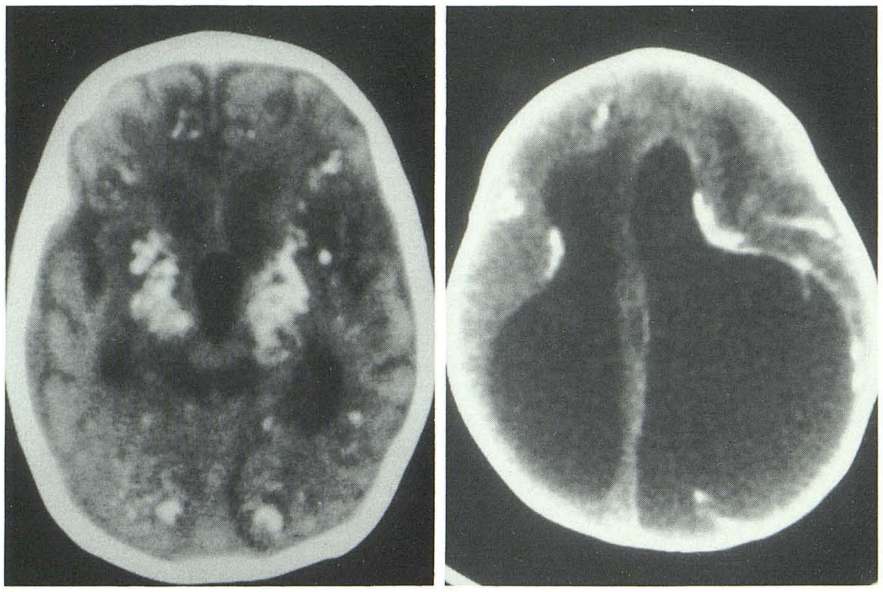

1 2

Fig. 3. CMV infection in a 11-week-old microcephalic retarded infant. Typical periventricular calcifications are present on CT. Although microcephalic, there is a superimposed hydrocephalus secondary to aqueductal stenosis.

Fig. 4. CMV infection in a 10-month-old infant with migration anomalies, microcephaly and spastic quadriplegia. CT reveals periventricular calcifications on the right and pachygyria of the frontal lobes, more easily seen on the left.

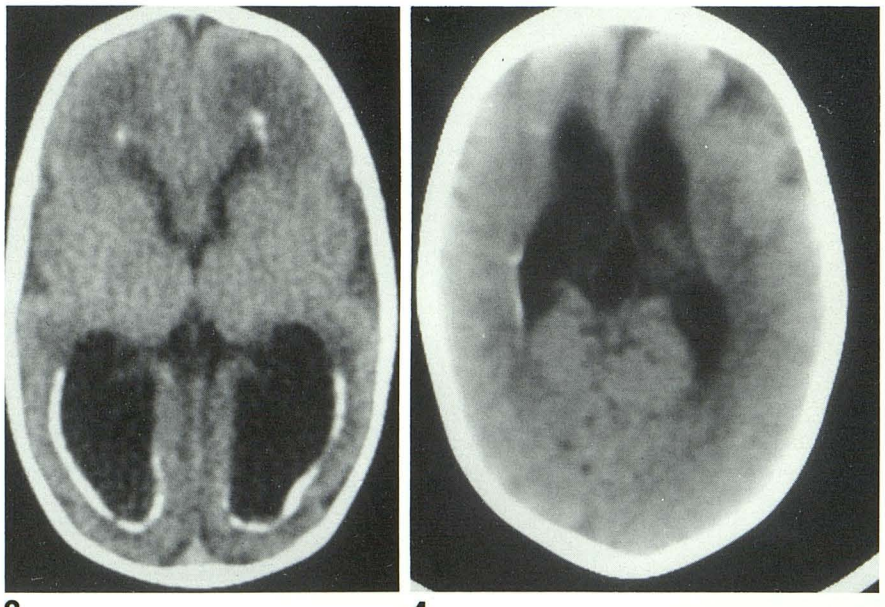

3 4

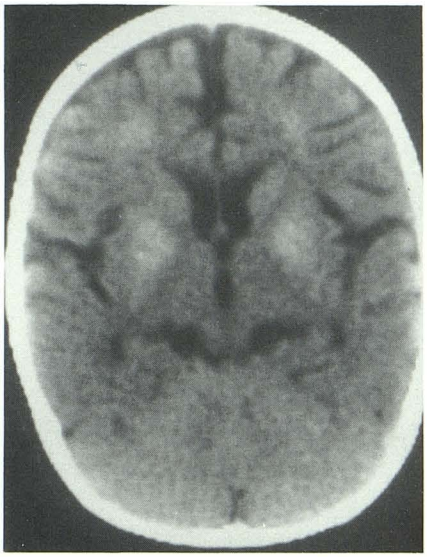

Fig. 5. AIDS; 15-month-old child with AIDS and delayed development; noncontrast CT. Typical calcifications are seen in the lenticular nuclei, the heads of the caudata nuclei, and more peripheral white matter in the frontal lobes. Generalized atrophy is also present.

Fig. 7. AIDS; T2-weighted MR (2800/80/.75) in a 20-month-old infant with developmental delay. Much of the subcortical white matter still has a higher signal than gray matter, indicating delayed myelination, particularly in the frontal lobes. The overall white matter volume is thought to be mildly decreased.

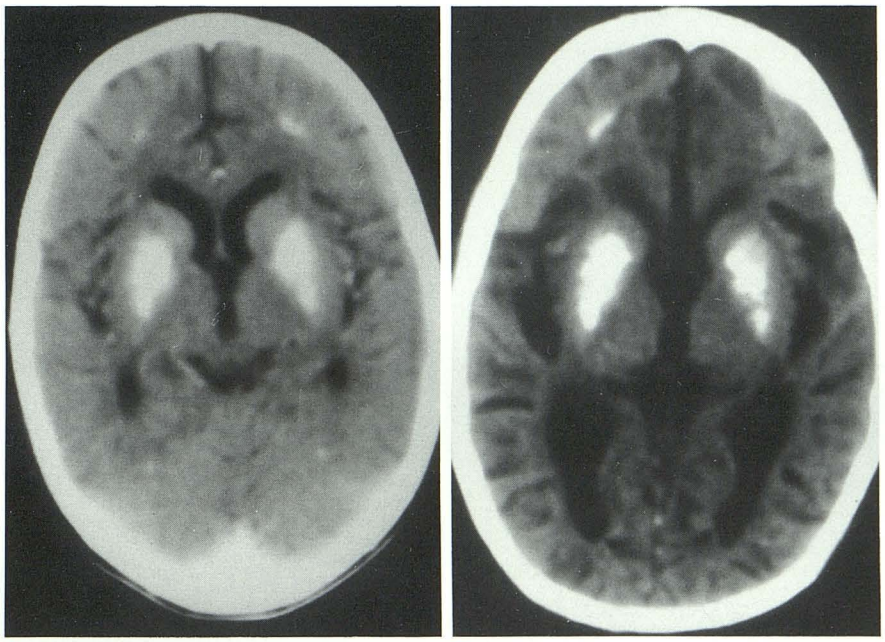

A B

Fig. 6. AIDS in a 3-year-old child.

A, Noncontrast CT shows dense calcifications in the basal ganglia and smaller but also dense calcifications in the frontal white matter. There is generalized atrophy.

B, Three weeks later, during a preterminal bout of sepsis without identifiable brain infection, CT shows striking further loss of brain tissue. The calcifications are unchanged.

imaging for CMV infection is 2.5 times more common than for toxoplasmosis. Like toxoplasmosis, CMV causes destructive changes in the brain that lead to calcification and microcephaly. CMV has a higher predilection for periventricular calcification (Fig. 3) that may be very thick in severe infections. Migration anomalies are sometimes associated with CMV infection (Fig. 4), suggesting a propensity to affect the germinal matrix. Calcification is also seen in the basal ganglia and other areas of the brain, so the pattern of calcification alone is not diagnostic.

Additional findings reported with CMV include: cerebellar hypoplasia (7), small subependymal cysts in the occipital horns that may be a fairly specific finding on MR (8), and increased echo-

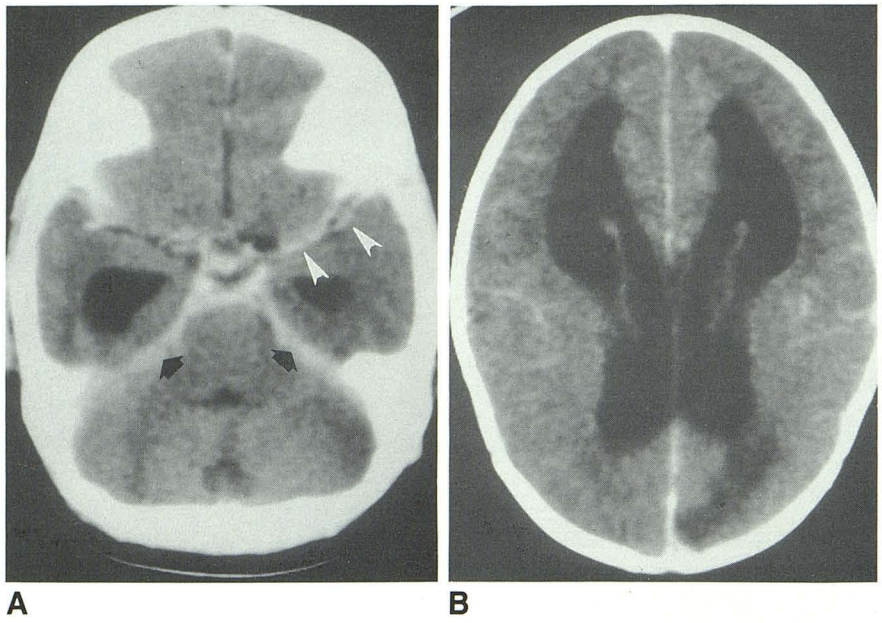

Fig. 8. Neonatal meningitis; 5-week-old infant with 1 week history of group B streptococcal meningitis.

A, Contrast-enhanced CT shows enhancement along the path of the middle cerebral artery (*arrow heads*), and the edges of the temporal lobes (*arrows*).

B, More superiorly, CT shows hydrocephalus and a right frontal infarction thought to be secondary to venous thrombosis.

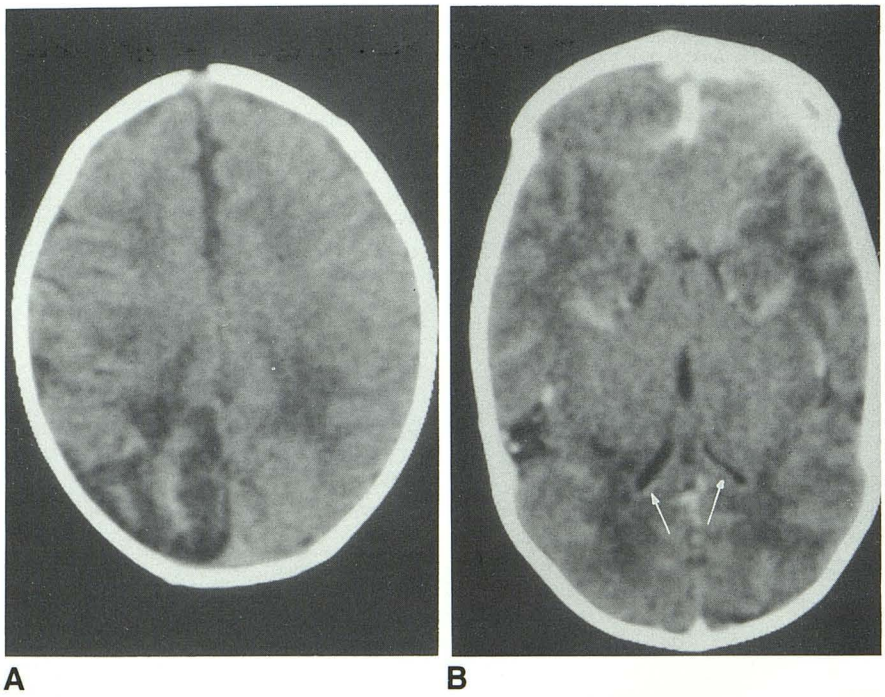

Fig. 9. Group B streptococcal meningitis; 6-week-old infant.

A, Noncontrast CT shows a hemorrhagic right occipital lobe infarct.

B, Contrast-enhanced CT shows faint enhancement of the ventricular wall (*arrows*), indicating ventriculitis.

genicity of the thalamo-striate arteries causing a candelabra-like pattern on ultrasound (9). However, Ben Ami et al (10) found the same candelabra-like pattern in a variety of congenital and neonatal infections. Tassin et al diagnosed CMV infection in the second trimester by using ultrasound to detect periventricular calcifications (11).

As calcifications are far less likely to be visible on MR than CT, CT is probably the more useful and the simpler examination to perform initially. MR may be needed if a migration anomaly is suspected but not clearly seen.

Clinically, infants infected with CMV are often premature with hepatosplenomegaly, jaundice, thrombocytopenia, and chorioretinitis. Sensorineural hearing loss is common (4). Perinatal infection is relatively common, but is rarely symptomatic.

Rubella

Because of maternal screening and immunization, congenital rubella has become a rarity in the developed world. Radiologic findings are similar to other viral infections. Microcephaly and brain calcification, especially basal ganglial and cortical calcification, are seen. Low density of the deep white matter has been described on CT (12). The first trimester infection is the most severe. The eyes are especially affected with cataracts, glaucoma, and chorioretinitis all occurring. Deafness is also common. Cardiac anomalies are also seen (13).

Herpes

Herpes simplex is far more often transmitted at birth than in utero. Reports of radiologic findings are rare. As with other placentally transmitted infections, herpes infection commonly causes microcephaly. Periventricular calcifications with ventricular enlargement and cortical calcifications are usually present (14, 15) but exhibit no distinguishing features. Retinal dysplasia is common.

Herpes zoster (chicken pox) is an uncommon intrauterine infection because of frequent childhood exposure and immunization. No reports of CT findings are published, but one would expect abnormalities similar to the previously described infections. Microcephaly, cataracts, chorioretinitis, cortical atrophy, and limb atrophy are common clinical abnormalities (16).

Others

Human parvovirus B-19 has recently been discovered to cause a variety of conditions including fetal hydrops and death (17). Its prevalence and severity are poorly studied, but perhaps it is an important "Other" in the TORCH spectrum.

AIDS

Seventy-eight percent of childhood HIV infection is maternally transmitted, even though only about one-third of HIV positive mothers pass on the infection (18). Although infants are asymptomatic at birth and the chronic symptoms develop slowly over many months, the disease will be described with the congenital infections. Most often, the infants begin to show progressive developmental delay by 6 months, and are prone to repeated infections. Unlike adults, they stay

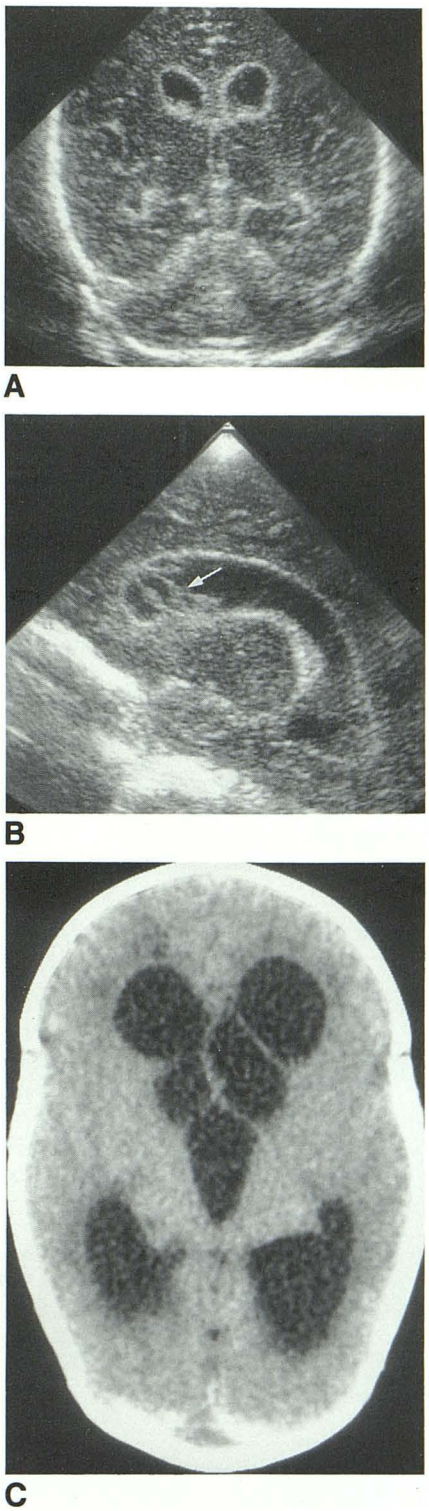

Fig. 10. Ventriculitis; *Listeria monocytogenes.*

A and *B*, 5 MHz coronal (*A*) and sagittal (*B*) sonograms at age 4 weeks show mild hydrocephalus with increased echogenicity of the ventricular walls and septations (*white arrow*) in the frontal horn.

C, Noncontrast axial CT at age 6 weeks confirms the frontal septations and shows progressive hydrocephalus.

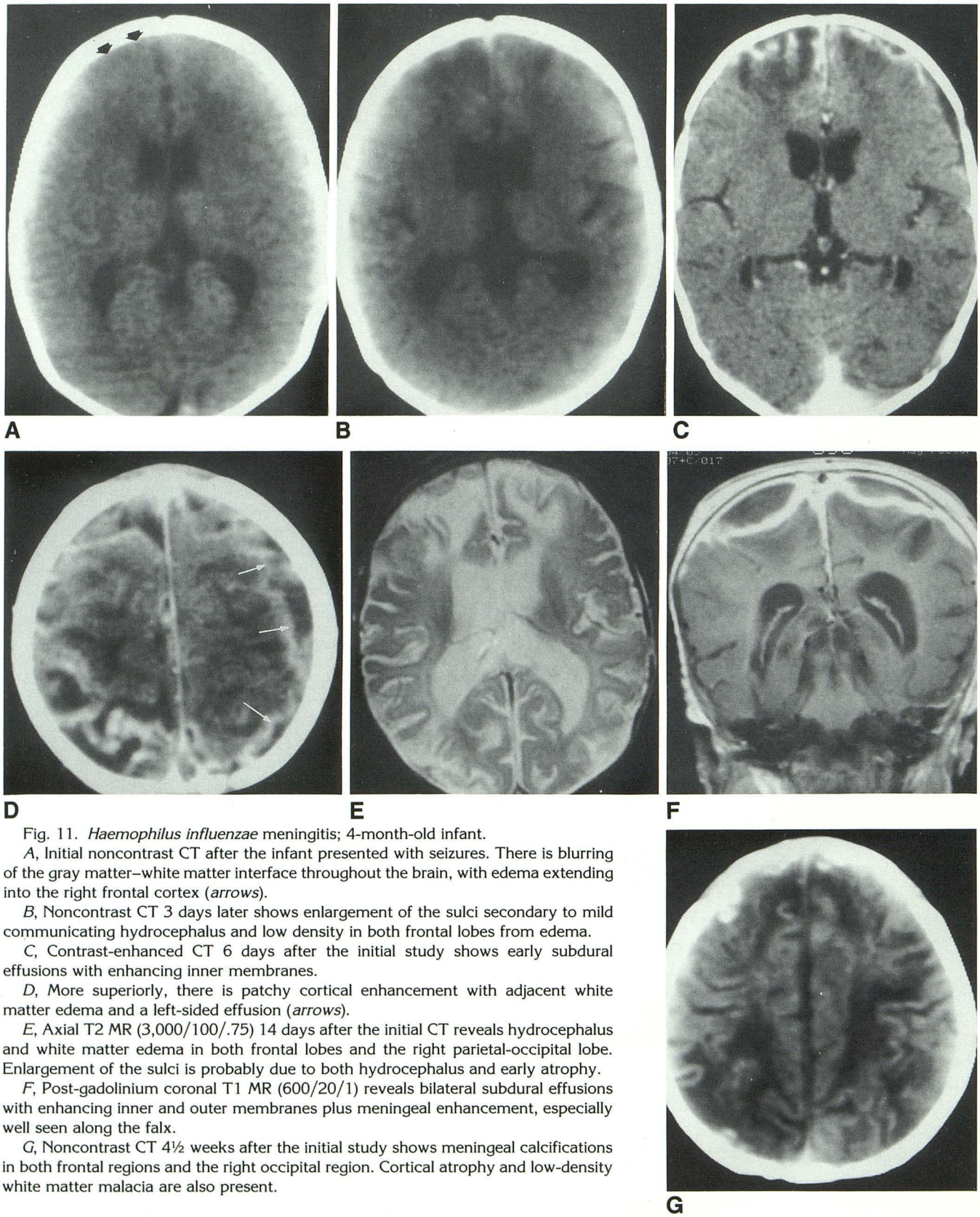

Fig. 11. *Haemophilus influenzae* meningitis; 4-month-old infant.

A, Initial noncontrast CT after the infant presented with seizures. There is blurring of the gray matter–white matter interface throughout the brain, with edema extending into the right frontal cortex (*arrows*).

B, Noncontrast CT 3 days later shows enlargement of the sulci secondary to mild communicating hydrocephalus and low density in both frontal lobes from edema.

C, Contrast-enhanced CT 6 days after the initial study shows early subdural effusions with enhancing inner membranes.

D, More superiorly, there is patchy cortical enhancement with adjacent white matter edema and a left-sided effusion (*arrows*).

E, Axial T2 MR (3,000/100/.75) 14 days after the initial CT reveals hydrocephalus and white matter edema in both frontal lobes and the right parietal-occipital lobe. Enlargement of the sulci is probably due to both hydrocephalus and early atrophy.

F, Post-gadolinium coronal T1 MR (600/20/1) reveals bilateral subdural effusions with enhancing inner and outer membranes plus meningeal enhancement, especially well seen along the falx.

G, Noncontrast CT 4½ weeks after the initial study shows meningeal calcifications in both frontal regions and the right occipital region. Cortical atrophy and low-density white matter malacia are also present.

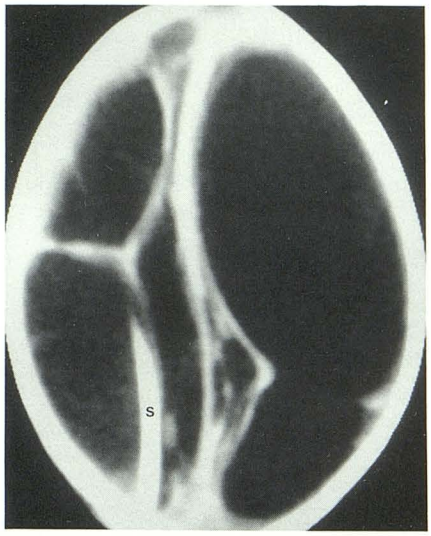

Fig. 12. Hydrocephalus with septations; 2-month-old infant. Contrast-enhanced CT through the lateral ventricles shows enhancement of multiple septations and of the ventricular walls. The fluid compartments have differing densities due to variable protein content. A portion of the ventricular shunt (*s*) is visible on the right side. There is a shift of the midline structures to the right, because of noncommunication on the left.

Fig. 13. Citrobacter infarction; contrast-enhanced CT in a 24-day-old infant. There is a large homogeneously low-density mass with enhancing rim in the right frontal lobe resembling an early abscess. The mass expanded even larger, but was a sterile necrotic infarction at operation.

relatively free of obvious central nervous system (CNS) complications, such as unusual tumors and infections.

Imaging studies are likely to show atrophy and calcification. In a group of 29 children studied at the author's hospital, 25 of whom had neurologic deterioration, 26 (89%) had atrophy, especially centrally. Ten (34%) had calcification of the basal ganglia (Figs. 5 and 6). White matter calcification was also seen in three of these children (Figs. 5 and 6) and cerebellar calcification in one. All 10 children were symptomatic and at least 12 months old. MR revealed delayed white matter myelination, increased T2 signal in the white matter, and suspicion of decreased white matter volume (Fig. 7) (19). The latter finding might also be related to maternal drug use itself, which has been reported to cause white matter hypoplasia (20).

Opportunistic infections such as toxoplasmosis, common in adults, are found much less often in children. Reactivation of congenital CMV has been reported (21). Active viral infection of the deep white matter is common (22). Brain-stem encephalitis has been reported (23).

Three children in our series had intracerebral hemorrhage secondary to thrombocytopenia. Park et al 24 found a 24% incidence of hemorrhagic and/or nonhemorrhagic infarcts at autopsies of pediatric AIDS patients. Additionally, one child had an arteropathy and another had marked dilatation of the circle of Willis. CNS tumors are uncommon in pediatric AIDS. Scattered cases of non-Hodgkin lymphoma are documented (25).

Perinatal and Early Infancy Infection

Neonatal sepsis is very dangerous, with a mortality rate of 15%–50% (26). Bacterial meningitis is likewise devastating. Group B streptococcus, gram negative *Enterobacter* bacilli, and *Listeria monocytogenes* are the three most common causes of neonatal meningitis (26).

Sepsis occurs in 1.5 per 1,000 births (27), and meningitis in 20% of these. Infections occurring in the first days of life are likely to be maternally transmitted; those occurring after a few days are not (28). The route of infection is thought to be hematogenous, probably with choroid plexus involvement and ventriculitis being the intracranial origin of the infections.

Imaging studies are usually not specific for individual infections. However, Volpe (28) emphasizes some pathologic variables that may be reflected in imaging. He indicates effusions are much less common in meningitis occurring in the first week of life than 2 or 3 weeks later. Group B streptococcal infection has a more limited inflammatory reaction in the brain, but a higher incidence of infarctions.

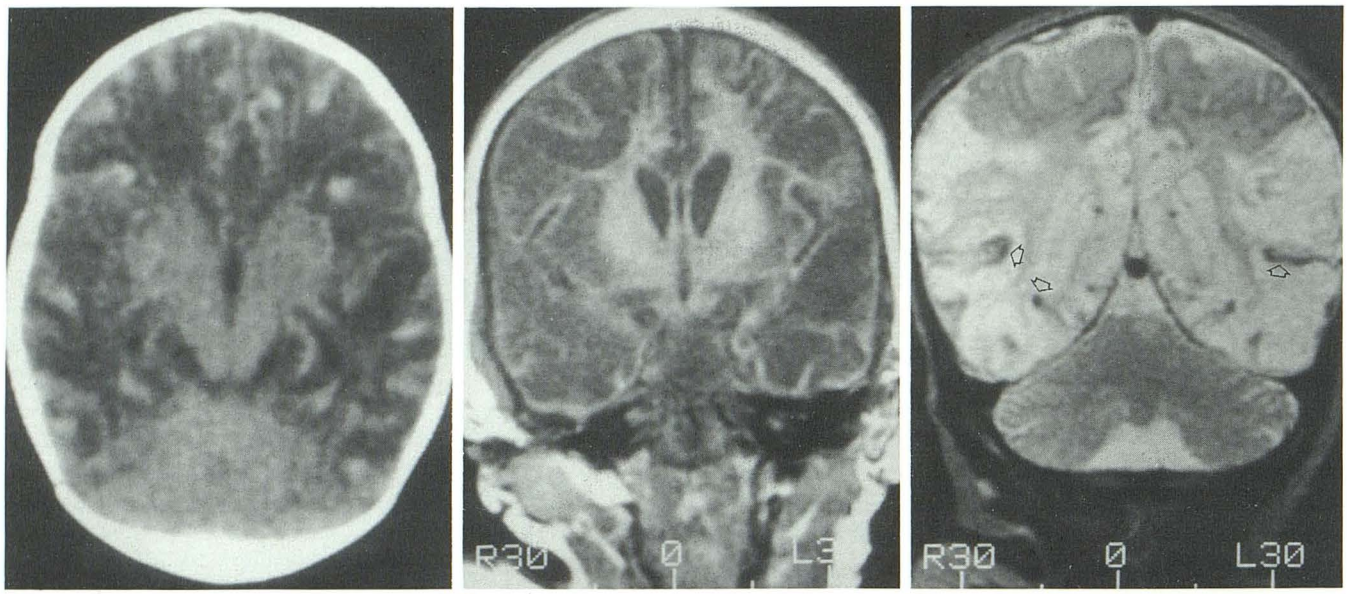

Fig. 14. Herpes encephalitis; 4-week-old infant.

A, Noncontrast CT. The broad zone of low density throughout much of the cerebral hemispheres from cortex to external capsule contains multiple "gyral" high densities thought to represent hemorrhage.

B, Coronal T1 MR (600/20/2) 4 days later shows diffuse low-signal edema throughout most of the brain, with some cortical and central sparing.

C, Coronal T2 MR (3600/100/1) through the parietal lobes. High-signal edema spares only the superior part of the parietal lobes. Multiple low-signal foci in the cortex (*arrows*) are due to hemorrhage.

Arachnoiditis is often basal (Fig. 8). Thrombosis from venous infarction is relatively common (Figs. 8 and 9). Ventriculitis occurs in 50% or more of cases (29), but is usually not obvious on imaging studies (Fig. 9). It can sometimes be identified on ultrasound exams (30) with increased intraventricular echoes from inflammatory debris, thickened irregular ventricular walls, periventricular echoes, and parenchymal cavitation when severe (Fig. 10).

Imaging studies may change rapidly from initial meningitis to severe edema in a few days, and to multiple infarcts, atrophy, or encephalomalacia within 2 to 3 weeks (Fig. 11). Calcification has been reported as early as 4 to 5 weeks after infection (31, 32) and may vary in location from periventricular to meningeal (Fig. 11G). Hydrocephalus is common, probably resulting from both arachnoiditis and ventriculitis (Figs. 8 and 11). Multiple isolated ventricular septations may occur, making shunting of the hydrocephalus more complicated (Fig. 12). Increased echogenicity of the parenchyma may be displayed by ultrasound (33), but such echogenicity may indicate edema, hemorrhage, and/or infarction. Babcock and Han (34) suggested increased gyral echoes are a precursor to infarctions and suggest poor outcome.

Citrobacter organisms in particular, and other gram negative bacilli that secrete endotoxins have a propensity to cause large focal cavitated infarcts, often with abscess formation (35). Subdural effusions are common in neonatal infections, especially with gram negative meningitis, and, according to Volpe (28), after the first week. These effusions may be sterile or infected (Fig. 13).

While the specificity and accuracy of brain pathology generally increases from ultrasound to CT to MR, infants may be far too ill to undergo a long MR. Even through ultrasound may be a less specific method, many abnormal findings can be identified, and the outcome worsens for the increased frequency of such findings.

Neonatal herpes infection is almost always herpes simplex II from maternal vaginal transmission at birth. The incidence is said to be about 1 per 2,000–5,000 births (36, 37). Focal seizures are commonly the first symptoms. Involvement is diffuse throughout the cerebrum. Cerebellar involvement has been reported in about half of the cases (36). Diffuse but patchy gray matter and

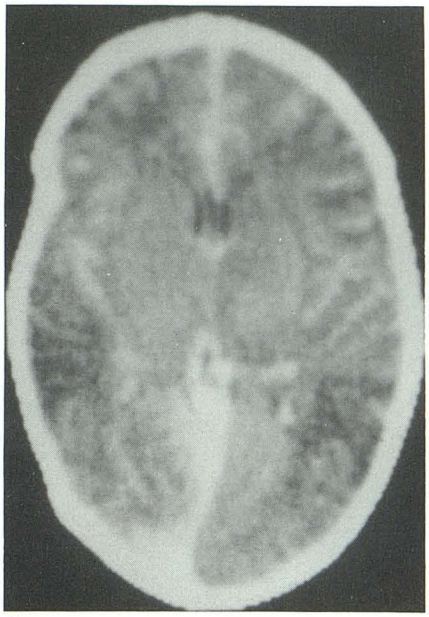

A

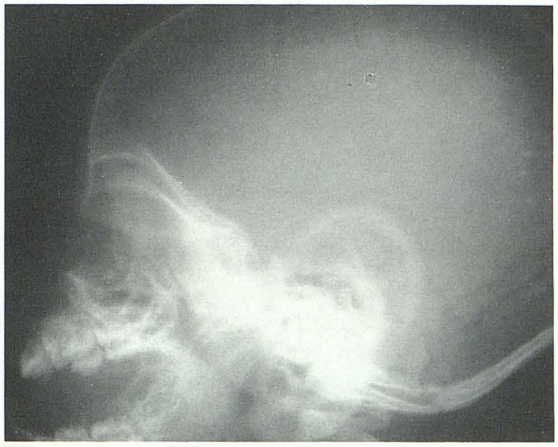

B

Fig. 15. Herpes encephalitis.

A, Contrast-enhanced CT during acute infection shows low density throughout the frontal and posterior cerebral regions, with increased brightness to the gyri.

B, Lateral skull radiograph 6½ months later shows microcephaly and multiple intracranial calcifications.

white matter attenuation and signal changes (edema) are often the first CT or MR findings, with later meningeal enhancement visible by both exams (Figs. 14 and 15). CT scans are usually not positive in the first 24 to 48 hours, but Norbehesht et al (36) found three of 15 infants had positive CT scans within 1 day after symptoms began. Increased gyral density and gyral enhancement may develop quickly (Fig. 14), possibly representing hemorrhage or calcification (36, 38). I believe that the early increased density is more likely hemorrhage secondary to reperfusion, although calcification clearly occurs later (36) (Fig. 15). Similar gyral increased densities and increased T2 MR signal is seen in other infections and in anoxic infants. Junck et al (39) reported an infant in whom persistent high density on CT was shown to be due to contrast retained in the brain, at least in part.

While other viral encephalitis is uncommon in the neonatal period, Haddad et al (40) reported a case of neonatal echovirus infection with periventricular white matter necrosis. Unfortunately, no early MR was done to prove the finding did not exist prior to the infection.

Infection in Later Infancy

Beyond the neonatal period, bacterial meningitis frequently remains a devastating illness with similar findings to the neonate. Subdural effusions remain common, especially with *Haemophilus influenza* infection (41) (Fig. 16). Probably due to the expandability of the infant head, indolent extradural and subdural empyemas may occasionally occur with few symptoms (42) (Fig. 17).

Infections beyond Infancy

As one might expect, the older the child, the more adult-like is the infection. Discussion of these diseases, therefore, will be relatively brief.

Meningitis

Meningitis is usually milder in older children than in infants. These children often do not undergo imaging except for a CT prior to lumbar puncture. This CT almost invariably shows no obstructive abnormality. Mild hydrocephalus is common. Enhancement is often not visible on CT. In the author's hospital, only 42% of contrast-enhanced CT scans revealed any enhancement. MR is more likely to reveal meningeal enhancement (Fig. 18), as has been experimentally documented (43).

Encephalitis

HSV1 is the most commonly reported viral encephalitis. In older infants and children, as in adults, it usually affects the temporal-Sylvian region. Initial findings are focal edema and occasional hemorrhage on CT (44) (Fig. 19), and altered signal intensity in the temporal cortex and

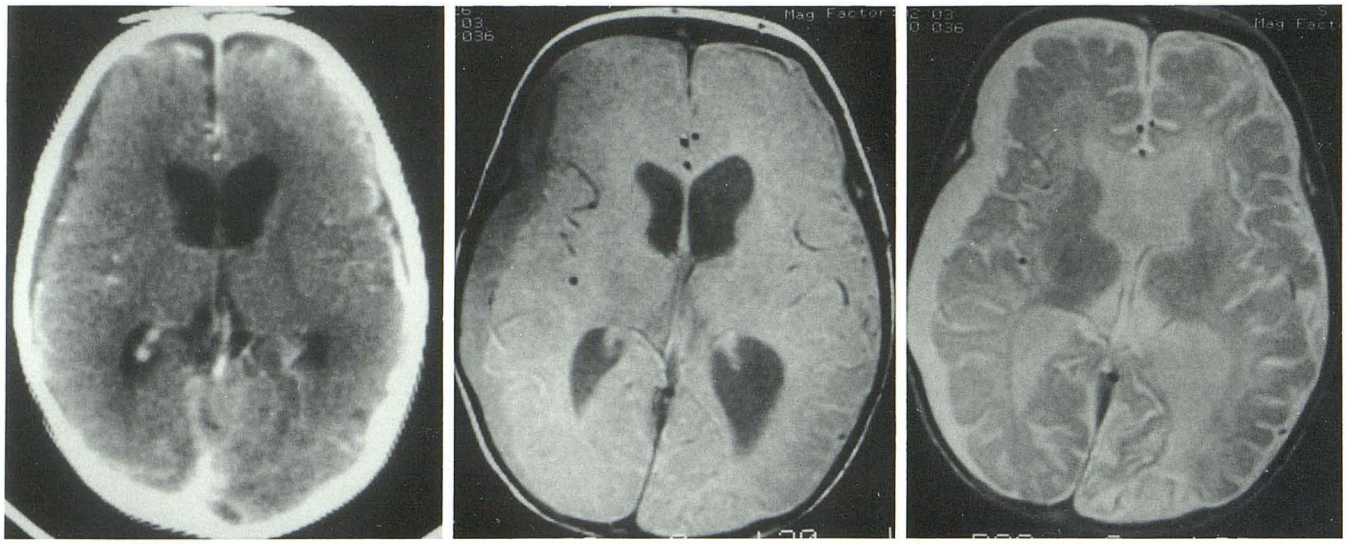

Fig. 16. *Haemophilus influenzae* meningitis with subdural effusion; 7-month-old infant.

A, Contrast-enhanced CT shows bilateral effusions with prominent enhancement on the left side and hydrocephalus.

B, Proton-density MR 2 weeks later (2800/30/1). The effusion is larger, especially on the right, exerts mass effect, and has a signal intensity greater than that of ventricular CSF. The higher protein content of the left-sided effusion causes an MR signal closer to that of brain, so it is better seen on T2 MR (2800/80/1) (*C*) where the full extent of the effusion is more easily recognized.

white matter on MR (Fig. 20). Subsequent infarct or atrophy is common. Calcification has been reported on long-term follow-up in children less than 3 years old (44). The temporal location is fairly specific for HSV1. Diffuse cerebral involvement does occur (45) and brain-stem encephalitis is occasionally reported (46). CT is rarely positive before 48 hours after onset of neurologic symptoms. Radionuclide brain scan may be a positive earlier (47). MR may also be abnormal earlier.

Other viral encephalitides occur, but are often the diagnosis of exclusion (Fig. 21). Epstein-Barr infection has recently been found to cause rapidly changing multifocal gray matter and white matter abnormalities on MR (48).

Postinfectious Encephalitis

Subacute sclerosing panencephalitis (SSPE) is a progressive encephalitis found primarily in children several years after measles infection. It is rare, with an incidence said to be 1 per million (49). Onset is usually heralded by mental deterioration, behavior problems, and seizures with a usually fatal outcome months to years later. Destruction of both cortical gray matter and white matter and brain stem occur. White matter demyelination and white and gray matter gliosis occur (50). Recently, measles virus genomic sequences have been grown from SSPE brain-tissue samples (51).

CT is often initially normal, followed by diffuse atrophy with relapses (52, 53), with marked enlargement of the Sylvian fissures. Multiple low densities may appear in the white matter (54) plus enhancement of subcortical white matter and corpus callosum (53). MR has shown extensive cerebral and cerebellar white matter and brain-stem changes before CT is positive (50). Weiner et al (55) reported partial resolution of these changes in spite of clinical progression.

Acute disseminated encephalomyelitis usually occurs after a vaccination or a viral illness, or, sometimes, rheumatic fever. It is thought to be an autoimmune inflammatory encephalitis. Children usually present with seizures. There is often complete recovery. MR shows some multiple cortical and subcortical lesions with increased signal on T2-weighted images (Fig. 22) (56). CT has been reported to show decreased density in the white matter, with multiple nodular or gyriform areas of enhancement (57). The lesions may resemble multiple sclerosis.

Progressive multifocal encephalopathy (PML) is a demyelinating illness caused by reactivation of papovavirus. It is found in immune-suppressed patients, especially those with AIDS (58). MR shows much variability from focal single lesions to large confluent foci of increased T2 signal in the white matter, and even cortical involvement (59). There are no imaging reports of HIV positive children with PML.

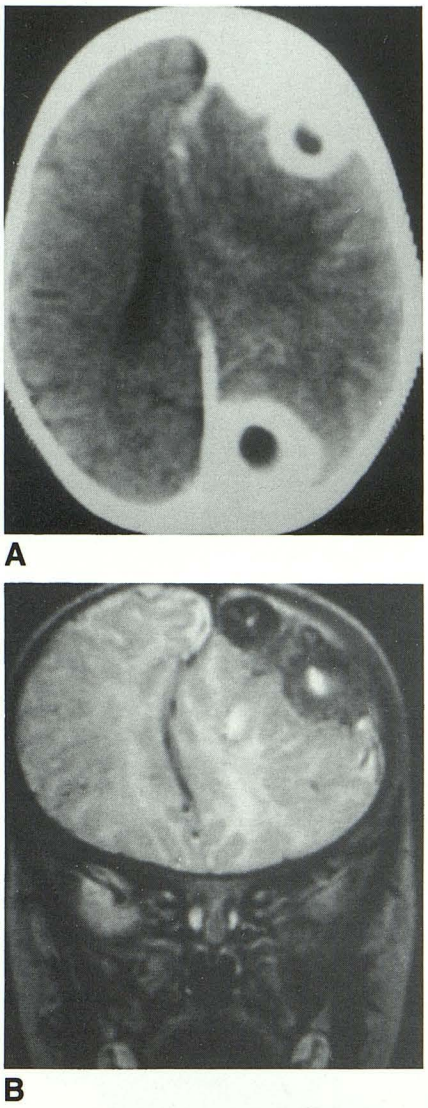

Fig. 17. Extradural empyema; 17-month-old girl referred for large head and developmental delay.

A, Contrast-enhanced CT shows extremely thick, enhancing walls of the frontal and occipital portions of the extradural empyema.

B, Noncontrast coronal T2 MR through the frontal lobes (2800/80/1) reveals the surface location of the collection. The thick walls have low signal and were found to be extremely fibrous at operation. The lesion extended in a tubular fashion across the cerebrum from frontal to occipital lobes with considerable mass effect.

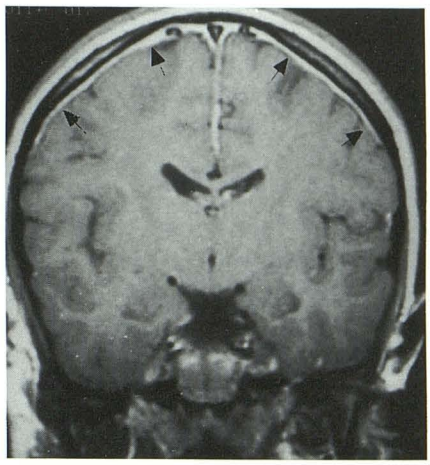

Fig. 18. Meningitis. Coronal post-gadolinium T1 MR (700/20/2) in a 13-year-old with X-linked hypogammaglobulinemia and viral meningitis. There is enhancement of the upper half of the meninges (*arrows*).

Subdural and Epidural Empyemas

Although occasionally due to craniotomy or trauma, nearly all empyemas in children are secondary to extension of frontal sinusitis, and, therefore, rarely occur before about age 10. Mastoiditis causes empyemas much less often than does sinusitis. CT reveals crescentic or biconvex lens-shaped fluid collections with decreased density and an enhancing rim (Fig. 23) (60). Although beginning frontally, they may spread quickly over any portion of the brain surface and between the hemispheres. Except for the midline location, it may be difficult to tell if the infection is subdural or epidural. However, with MR a displaced dark dural rim can be identified in epidural empyema (61). The fluid has increased signal compared to water in both T1 and T2. Cortical edema and cerebritis are more easily seen on MR than on CT.

Abscesses

Bacterial abscesses are rare in childhood in developed countries, even in children with congenital heart disease and immune problems. The exception is the neonatal infections previously described. Abscesses evolve from focal cerebritis with formation of a fibrous capsule. Enzman et al (62, 63) described four stages—early and late cerebritis, and early and late capsule formation. The process takes 2 weeks from onset. True capsule formation is difficult to determine by CT. As the capsule forms, there is enhancement by either exam (Figs. 24 and 25). MR is said to have a slightly increased T1 and decreased T2 signal early, and an increased T2 signal as the capsule matures. In the chronic phase, there is a decreased T2 and an isointense T1. Surrounding edema is usually intense.

Rings of variable density have been described within the central necrosis (62). Extraparenchymal spread to the ventricles and subarachnoid space is said to be more commonly seen with MR than CT (64). Although the appearance of

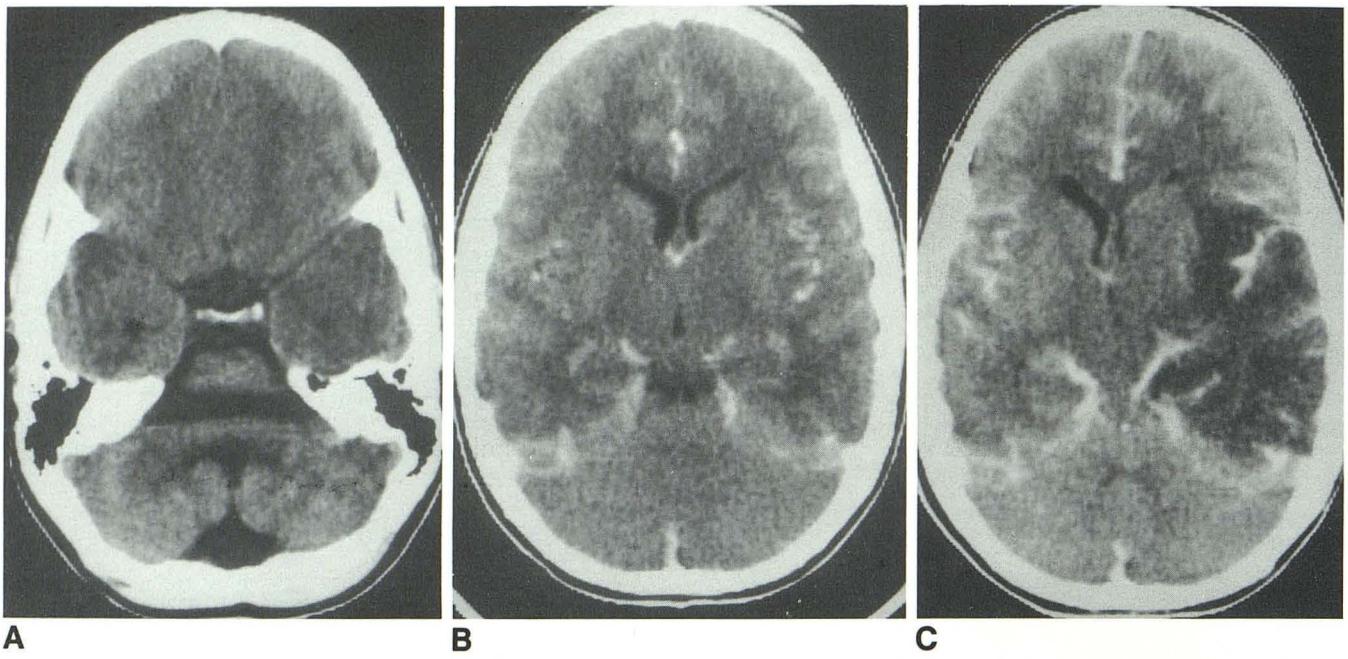

Fig. 19. Herpes encephalitis; 11-year-old boy with 1 day of headache and generalized seizure immediately before CT.
A, Noncontrast CT shows questionably decreased density in the left temporal lobe.
B, Contrast-enhanced CT interpreted as normal, but perhaps showing abnormal prominence of left Sylvian fissure arteries.
C, Contrast-enhanced CT 6 days later shows marked edema of the left temporal lobe.

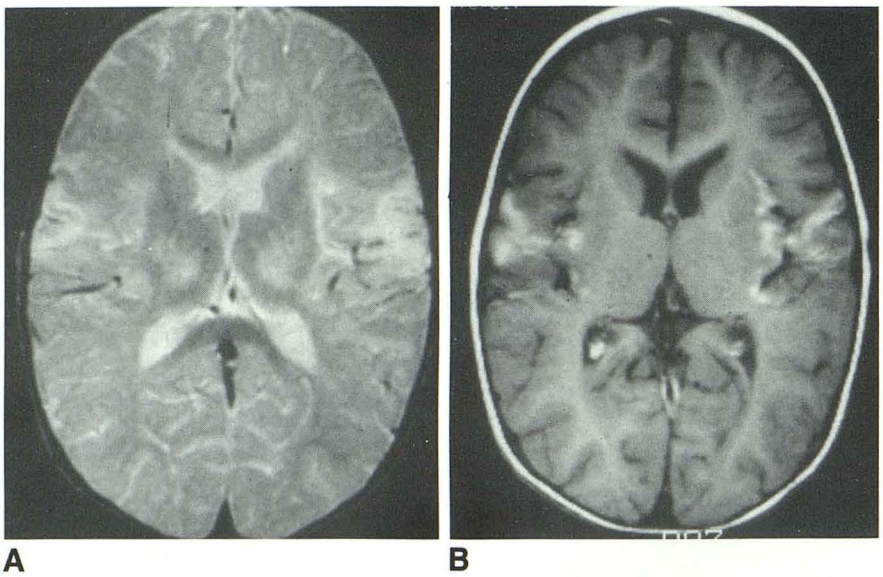

Fig. 20. Herpes encephalitis; 1-year-old infant.
A, Axial T2 MR (2800/80/1) shows bilateral high signal in the temporal lobes, primarily cortical. The thalami and basal ganglia are also affected.
B, Contrast-enhanced axial T1 MR (620/30/2) at the same level shows enhancement of the temporal-opercular cortex on each side.

abscesses in children is not significantly different from that in adults, the agents of infection often differ. Brook (65) reported 63% anaerobic, 26% mixed, and only 11% aerobic infections in 19 pediatric abscesses and empyemas. Sinusitis was common in abscesses as well as empyema.

Granulomatous Disease

Tuberculosis is relatively rare in developed countries, but is common throughout the rest of the world. Tuberculomas are said to account for 47% of intracranial masses below age 15 in India (66). Neurologic symptoms are often mild. Miliary tuberculosis is usually the primary source of CNS seeding. Basal meningitis is typical (Fig. 26), with the exudate sometimes causing vasculitis and infarcts due to occlusion of the penetrating arteries (67). Tuberculomas may occur in any part of the brain. MR appearance is typical, being isotense to gray matter on both T1 and T2 images, although occasionally being hypointense on T2.

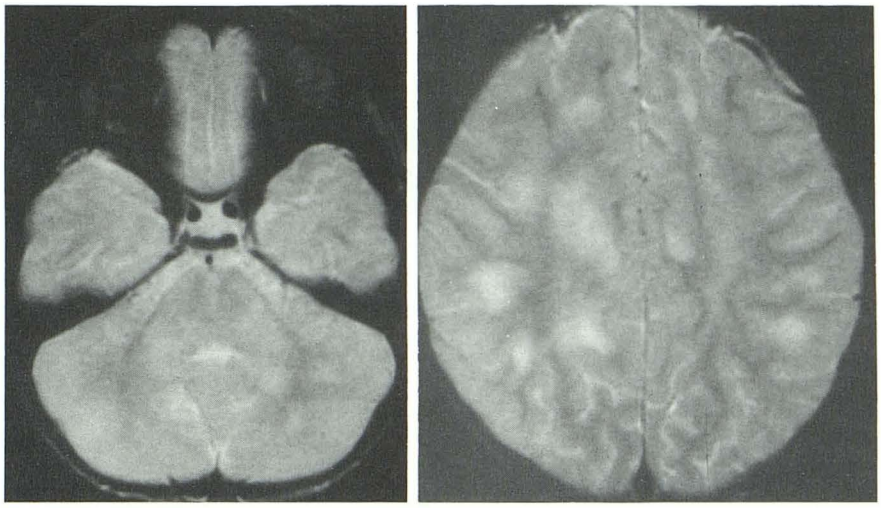

Fig. 21. Viral encephalitis; 2-year-old boy; T2 MR (2800/80/1).

A, Mildly increased signal is visible in the brain stem, cerebellar peduncles, and cerebellar white matter.

B, Focal increased signal is more evident in the subcortical white matter. There was minimal enhancement. Follow-up study showed complete reversal, suggesting the findings were due to edema.

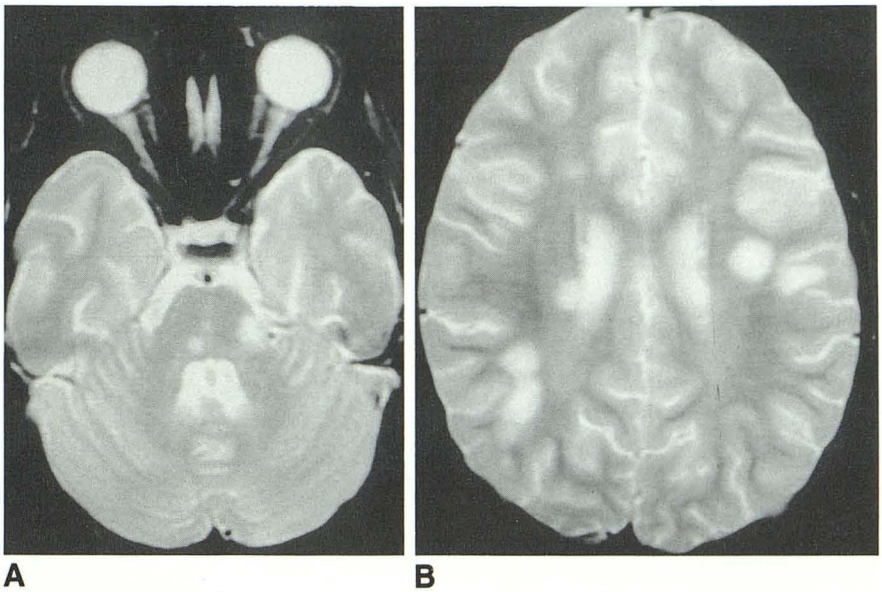

Fig. 22. Acute disseminated encephalomyelitis in a 6-year-old; T2 axial MR (2200/80/1).

A, Foci of high signal are present in the brain stem.

B, Multiple foci of high signal demyelination are scattered throughout the white matter from subcortical to periventricular locations. (Case courtesy of Dr. Carl Geyer, Walter Reed Army Medical Center, Washington, DC.)

This is combined with a ring-like enhancement (68). Central calcification with ring enhancement is commonly seen on CT (69).

Sarcoidosis is a granulomatous disease of unknown cause. It is quite rare before puberty, and, therefore, is uncommon in children. Cranial neuropathy is common (70), and MR can identify enhancement of affected nerves. Meningitis and hydrocephalus are common. Parenchymal masses may be found, especially in the hypothalamus. The granulomas resemble those of tuberculosis, and have no surrounding edema (Fig. 27) (71).

Lyme Disease

Tick-borne Lyme disease, caused by the spirochete *Borrelia burgdorferi* occurs through multiple regions of North America. Neurologic symptoms are variable and nonspecific. Clinical diagnosis can be very difficult without the history of the characteristic large ring-like rash. MR has been reported to show involvement throughout many white matter areas from cerebral subcortical zones to the cerebellar peduncles (72, 73). Thalamic and basal ganglial regions may be involved. The lesion may show ring-like enhancement after Gd-DTPA (73).

Cysticercosis

Parasitic infections of the CNS are quite rare in North America except for cysticercosis which is caused by ingestion of ova from *Taenia solium* (the pork tape worm). Secondary larvae invade the CNS and other tissues. Nearly all pediatric

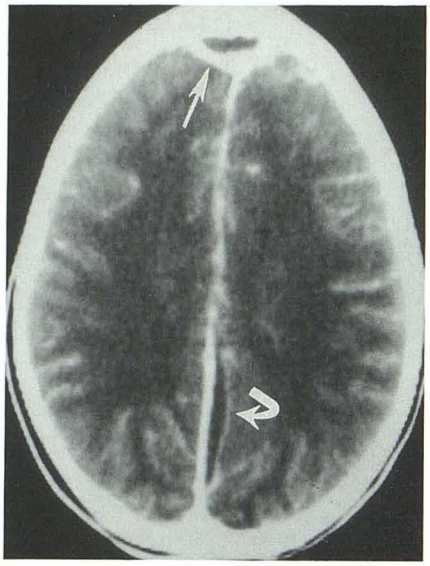

Fig. 23. Extra-dural empyema; 10-year-old girl with sinusitis and neurologic symptoms. Contrast-enhanced CT identifies frontal extradural abscess with densely enhancing dura (*arrows*) crossing the midline anteriorly. Subdural empyema is visible further posteriorly against the falx (*curved arrow*).

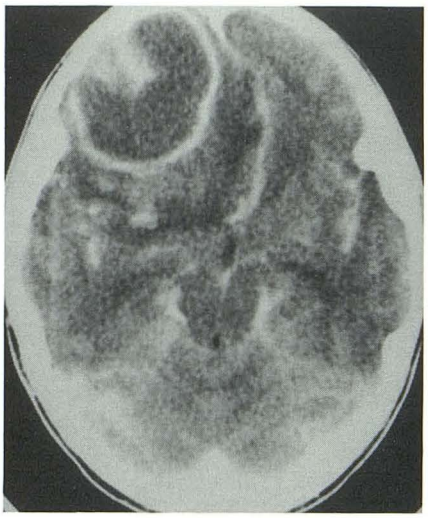

Fig. 24. Cerebral abscess; 10-year-old who presented with fever, seizure and an infected tooth. There was no sinusitis. Contrast-enhanced CT reveals an enhancing capsule and marked mass effect in the right frontal lobe. Pus was drained at operation. The cause for the enhancement within the capsule adjacent to the inner table was not identified at operation.

Fig. 25. Abscess; 15-year-old girl.

A, Sagittal T1 MR (800/25/2) without gadolinium. There is low signal within the abscess capsule. The capsule has higher signal than brain, and there is an irregular rim of low-signal edema.

B, Sagittal T2 MR (2500/80/2). The abscess contents and the edema all have increased signal. The material in the capsule that shows high T1 signal and low T2 signal is probably hemorrhage. The findings are compatible with a maturing abscess. (Case courtesy of Dr Larissa Bilaniuk, Children's Hospital of Philadelphia.)

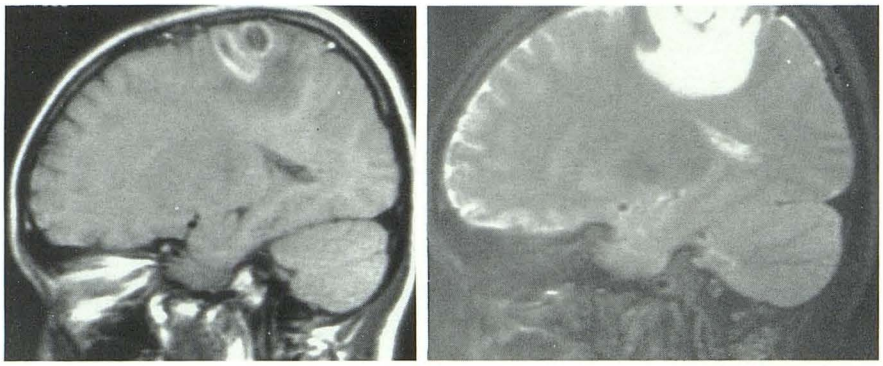

A B

cases occur in children who have emigrated from endemic areas of Mexico, Central, or South America. Most present with seizures. Symptoms are relatively rare before 6 years of age (74–76). In endemic areas, children often show multiple lesions that are spread from the subarachnoid space to the ventricles. Children emigrating from these areas to north Mexico usually have only one or a few foci of infection that are "parenchymal." Pathologically, many of the lesions that appear to be parenchymal by imaging are actually found to lie deep in sulci (77).

Kramer et al (75) described several clinical and pathologic phases with corresponding CT findings. These begin with nonspecific symptoms and a CT showing parenchymal edema without enhancement. This progresses to a small enhancing lesion that may have no edema. Chronic lesions first have cysts without enhancement or edema. The cysts then become edematous and go on to ring enhancement, as a fibrous capsule forms around the cyst (Fig. 28). The ring of enhancement corresponds pathologically to a dying larva. It is usually an average of 5–20 mm in diameter. By this time, most adults and children have seizures. Following this phase, an eccentric nodule on the cyst wall correlates with a dead or dying scolex. This is followed by calcification of the cyst wall. The changes occur over a number of months.

MR descriptions have been somewhat less specific. Suss et al (78) described live cysts with

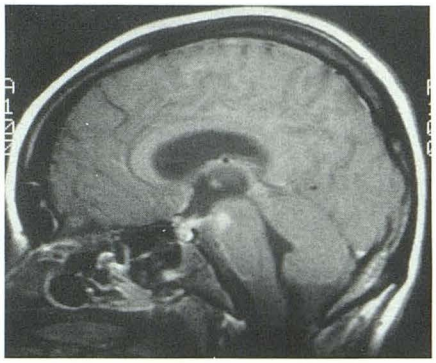

Fig. 26. Tuberculosis in a 15-year-old girl. Gadolinium-enhanced T1 MR (620/20/2) shows enhancement of the meninges along the belly of the pons, the midbrain, and beneath the hypothalamus with mild hydrocephalus.

Fig. 27. Sarcoid; 17-year-old black girl. Contrast-enhanced sagittal T1 MR (620/20/2) shows enhancement of the pituitary stalk and hypothalamus. No cranial nerve enhancement was identified.

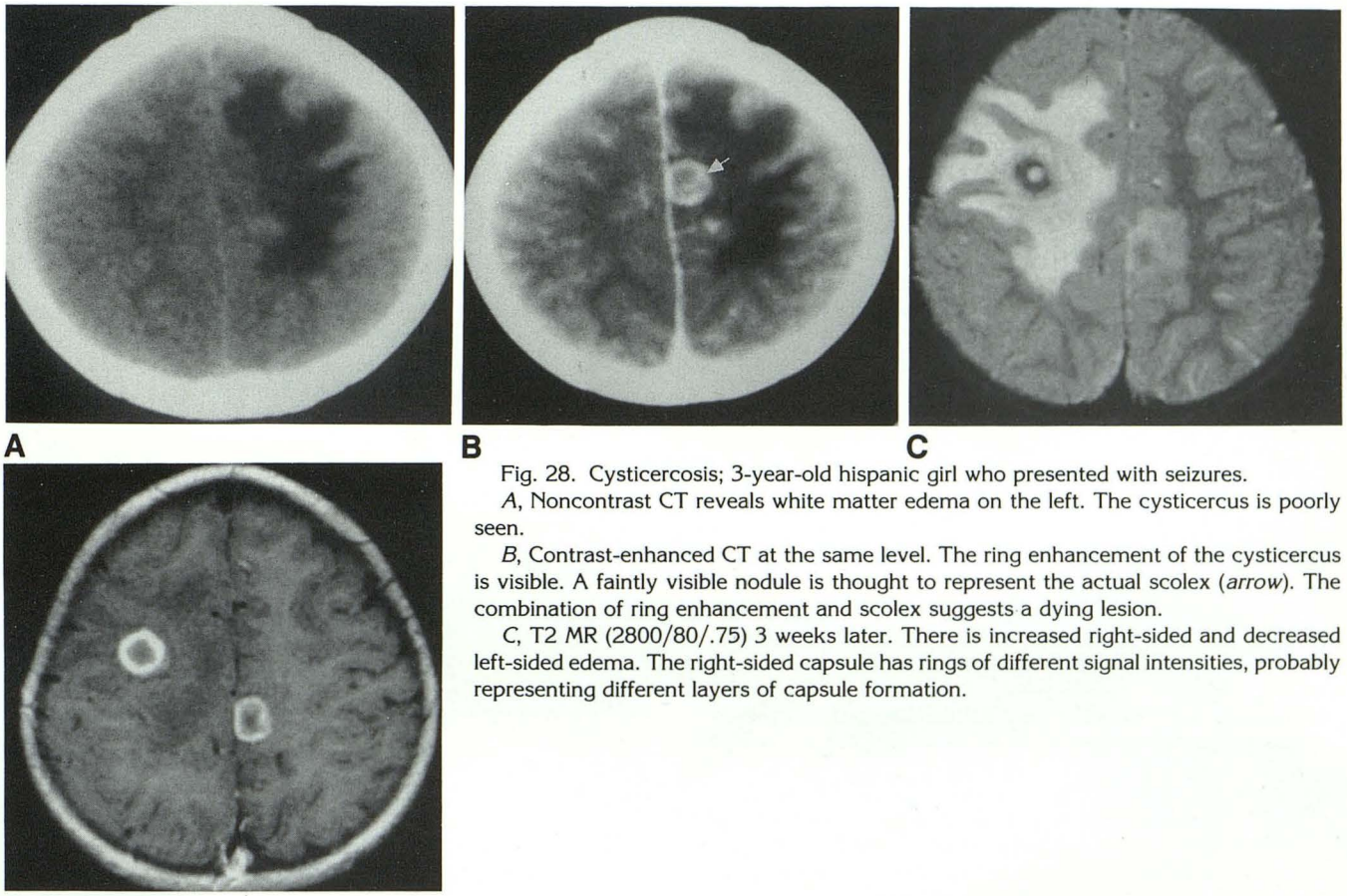

Fig. 28. Cysticercosis; 3-year-old hispanic girl who presented with seizures.

A, Noncontrast CT reveals white matter edema on the left. The cysticercus is poorly seen.

B, Contrast-enhanced CT at the same level. The ring enhancement of the cysticercus is visible. A faintly visible nodule is thought to represent the actual scolex (*arrow*). The combination of ring enhancement and scolex suggests a dying lesion.

C, T2 MR (2800/80/.75) 3 weeks later. There is increased right-sided and decreased left-sided edema. The right-sided capsule has rings of different signal intensities, probably representing different layers of capsule formation.

signal higher than cerebrospinal fluid (CSF) on long TR images, and dying cysts with signal lower than CSF on T1 images. Martinez (76) showed active cysts to have signal equal to CSF in T1 or T2 MR, whereas the scolex within the cyst has increased signal on both T1 and T2 images (Fig. 28C). Degenerating cysts lost the identifiable scolex, had a more irregular cyst shape, and less edema (Fig. 28D). This last stage or that of ring enhancement with edema suggests a dying scolex. Calcification indicates death of the parasite. MR better identifies the lesions than CT, except for those that are calcified, and also much more clearly shows nonparenchymal cysts.

References

1. Remington JS. The tragedy of toxoplasmosis. *Pediatr Infect Dis J* 1990;9:762–763
2. Diebler C, Dusser A, Dulac O. Congenital toxoplasmosis: clinical and neuroradiologic evaluation of the cerebral lesions. *Neuroradiology* 1985;27:125–130
3. Altschuler G. Toxoplasmosis as a cause of hydrencephaly. *Am J Dis Child* 1973;125:251–252
4. Stagno S. Significance of cytomegaloviral infections in pregnancy and early childhood. *Pediatr Infect Dis J* 1990;9:763–764
5. Stagno S, Pass RF, Cloud G, et al. Primary cytomegalovirus infection in pregnancy. *JAMA* 1986;256:1904–1908
6. Stagno S, Pass RF, Dworsky ME, Alford CA. Maternal cytomegalovirus infection and perinatal transmission. *Clin Obstet Gynecol* 1982;25:563–576
7. Urich H. Cerebellar malformations: some pathogenetic considerations. *Clin Exp Neurol* 1979;16:119–131
8. Boesch CH, Issakainen J, Kewitz G, Kikinis R, Martin E, Boltshauser E. Magnetic resonance imaging of the brain in congenital cytomegalovirus infection. *Pediatr Radiol* 1989;19:91–93
9. Toma P, Magnano GM, Mezzano P, Lazzini F, Bonacci W, Serra G. Cerebral ultrasound images in prenatal cytomegalovirus infection. *Neuroradiology* 1989;31:278–279
10. Ben-Ami T, Yousefzadeh D, Backus M, Reichman B, Kessler A, Hammerman-Rozenberg C. Lenticulostriate vasculopathy in infants with infections of the central nervous system: sonographic and Doppler findings. *Pediatr Radiol* 1990;20:575–579
11. Tassin GB, Maklad NF, Stewart RR, Bell ME. Cytomegalic inclusion disease: intrauterine sonographic diagnosis using findings involving the brain. *AJNR* 1991;12:117–122
12. Ishikawa A, Murayama T, Sakuma N, et al. Computed cranial tomography in congenital rubella syndrome. *Arch Neurol* 1982;39: 420–421
13. Weil ML. Infections of the nervous system. In: Menkes JH, ed. *Text book of child neurology*. Philadelphia: Lea & Febiger, 1985:316–431
14. Dublin AB, Merten DF. Computed tomography in the evaluation of herpes simplex encephalitis. *Radiology* 1977;125:133–134
15. Benator RM, Magil HL, Gerald B, Igarashi M, Fitch SJ. Herpes simplex encephalitis: CT findings in the neonate and young infant. *AJNR* 1985;6:539–543
16. Brunell PA. Varicella in the womb and beyond. *Pediatr Infect Dis J* 1990;9:770–772
17. Torok TJ. Human parvovirus B19 infections in pregnancy. *Pediatr Infect Dis J* 1990;9:772–776
18. Yogev R. Pediatric acquired immunodeficiency virus syndrome. *Pediatr Infect Dis J* 1990;9:767–768
19. Kauffman W, Civit CJ, Fitz CR, Rakusan T, Herzog K. CNS involvement in pediatric HIV infection: clinical-imaging correlation. *AJNR* 1992: (in press)
20. Dietrich RB, Shields WD, Sankar R. Cerebral white matter hypoplasia. Paper presented at the 76th annual meeting of the Radiological Society of North America, Chicago, November 1990.
21. Donovan Post MG, Curless RG, Gregorios JB, Scott GB, Sheldon JJ. Reactivation of congenital cytomegalic inclusion disease in an infant with HTLV-III associated immunodeficiency: a CT-pathologic correlation. *J Comput Assist Tomogr* 1986;10:533–536
22. Epstein LG, Sharer LR, Goudsmit J. Neurological and neuropathological features of human immunodeficiency virus infection in children. *Ann Neurol* 1988;23(suppl):S19–S23
23. Raphael SA, deLeon G, Sapin J. Symptomatic primary human immunodeficiency virus infection of the brain stem in a child. *Pediatr Infect Dis J* 1989;8:654–656
24. Park YD, Belman AL, Kim TS, et al. Stroke in pediatric acquired immunodeficiency syndrome. *Ann Neurol* 1990;28:303–311
25. Del Mistro A, Laverda A, Calabrese F, et al. Primary lymphoma of the central nervous system in two children with acquired immune deficiency syndrome. *Am J Clin Pathol* 1990;94:722–728
26. Klein JO. Bacteriology of neonatal sepsis. *Pediatr Infect Dis J* 1990; 9:778
27. Klein JO, Marcy SM. Bacterial sepsis and meningitis. In: Remington JS, Klein JO, eds. *Infectious diseases of the fetus and newborn infant*. Philadelphia: Saunders, 1990:601–644
28. Volpe JJ. Neurology of the newborn. In: *Bacterial and fungal intracranial infections*. Philadelphia: Saunders, 1987:596–632
29. Gilles FH, Jammes JL, Berenberg W. Neonatal meningitis: the ventricle as a bacterial reservoir. *Arch Neurol* 1977;34:560–562
30. Reeder JD, Sanders RC. Ventriculitis in the neonate: recognition by sonography. *AJNR* 1983;4:37–41
31. Chong-Wah A, Masel JP. Cerebral calcification following pseudomonas meningitis in an infant. *Aust Radiol* 1972;16:56–58
32. Kotagal S, Tantanasirivongse S, Archer CR. Periventricular calcification following neonatal ventriculitis. *J Comput Assist Tomogr* 1981; 5:651–653
33. Kotlus Rosenberg H, Levine RS, Stoltz K, Smith DR. Bacterial meningitis in infants: sonographic features. *AJNR* 1983;4:822–825
34. Babcock DS, Han BK. Sonographic recognition of gyral infarction in meningitis. *AJNR* 1985;6:119–122
35. Foreman SD, Smith EE, Ryan NJ, Hogan GR. Neonatal citrobacter meningitis: pathogenesis of cerebral abscess formation. *Ann Neurol* 1984;16:655–659
36. Noorbehesht B, Enzmann DR, Sullender W, Bradley JS, Arvin AM. Neonatal herpes simplex encephalitis: correlation of clinical and CT findings. *Radiology* 1987;162:813–819
37. Whitley RJ. NIAID Collaborative Antiviral Study Group. Interim summary of mortality in herpes simplex encephalitis and neonatal herpes simplex virus infections: vidarabine versus acyclovir. *J Antimicrob Chemother* 1983;12:105–112
38. Herman TE, Cleveland RH, Kushner DC, Taveras JM. CT of neonatal herpes encephalitis. *AJNR* 1985;6:773–775
39. Junck L, Enzmann DR, DeArmond SJ, Okerlund M. Prolonged brain retention of contrast agent in neonatal herpes simplex encephalitis. *Radiology* 1981;140:123–126
40. Haddad J, Messer J, Gut JP, Chaigne D, Christmann D, Willard D. Neonatal echovirus encephalitis with white matter necrosis. *Neuropediatrics* 1990;21:215–217
41. Martin LD, Kaplan AM, Rudinsky MF, Frost MD. Haemophilus influenzae meningitis with prolonged hospital course. *Pediatr Neurol* 1990; 6:260–264
42. Raghav B, Goulatia RK, Gupta AK, Misra NK, Singh M. Giant subdural empyema in an infant. *Neuroradiology* 1990;32:154–155
43. Matthews VP, Kuharik MA, Edwards MK, D'Amour PG, Azzarelli B, Dreesen RG. Gd-DTPA-enhanced MR imaging of experimental bacterial meningitis: evaluation and comparison with CT. *AJNR* 1988;9: 1045–1050
44. Sugimoto T, Woo M, Okazaki H, et al. Computed tomography in young children with herpes simplex virus encephalitis. *Pediatr Radiol* 1985;15:372–376
45. Zimmerman RD, Russell EJ, Leeds NE, Kaufman D. CT in the early diagnosis of herpes simplex encephalitis. *AJR* 1980;134:61–66
46. Robb L, Butt W. Brain stem encephalitis due to herpes simplex virus. *Aust Paediatr* 1989;25:246–247
47. Go RT, Yousef MMA, Jacoby CG. The role of radionuclide brain imaging and computerized tomography in the early diagnosis of herpes simplex encephalitis. *J Comput Tomogr* 1979;8:286–296
48. Tolly TL, Wells RG, Sty JR. MR features of fleeting CNS lesions associated with Epstein-Barr virus infection. *J Comput Assist Tomogr* 1989;13:665–668
49. Jabbour JT, Duenas DA, Sever JL, Krebs H, Horta-Barbosa L. Epidemiology of SSPE. *JAMA* 1972;220:959–962
50. Tsuchiya K, Yamauchi T, Furui S, Suda Y, Takenaka E. MR imaging

vs CT in subacute sclerosing panencephalitis. *AJNR* 1988;9: 943–946
51. Godec MS, Asher DM, Swoveland PT, et al. Detection of measles virus genomic sequences in SSPE brain tissue by the polymerase chain reaction. *J Med Virol* 1990;30:237–244
52. Manabe Y, Ono Y, Okuno T, Ueda T. Serial CT scans in subacute sclerosing panencephalitis. *Comput Tomogr* 1981;5:25–30
53. Modi G, Campbell H, Bill P. Subacute sclerosing panencephalitis. *Neuroradiology* 1989;31:433–434
54. Duda EE, Huttenlocher PR, Patronas NJ. CT of subacute sclerosing panencephalitis. *AJNR* 1980;1:35–38
55. Winer JB, Pires M, Kermode A, Ginsberg L, Rossor M. Resolving MRI abnormalities with progression of subacute sclerosing panencephalitis. *Neuroradiology* 1991;33:178–180
56. Barkovich AJ. *Pediatric neuroimaging: metabolic and destructive brain disorders.* New York: Raven Press, 1986;3:35–76
57. Thajeb P, Chen ST. Cranial computed tomography in acute disseminated encephalomyelitis. *Neuroradiology* 1989;31:8–12
58. Aksamit AJ, Gendelman HE, Orenstein JM, Pezeshkpour GH. AIDS-associated progressive multifocal leukoencephalopathy (PML): comparison to non-AIDS PML with a situ hybridization and immunohistochemistry. *Neurology* 1990;40:1073–1078
59. Mark AS, Atlas SW. Progressive multifocal leukoencephalopathy in patients with AIDS: appearance on MR images. *Radiology* 1989; 173:517–520
60. Zimmerman RD, Leeds NE, Danziger A. Subdural empyema: CT findings. *Radiology* 1984;150:417–422
61. Weingarten K, Zimmerman RD, Becker RD, Heier LA, Haimes AB, Deck MDF. Subdural and epidural empyemas: MR imaging. *AJNR* 1989;10:81–87
62. Enzmann DR, Britt RH, Yeager AS. Experimental brain abscess evolution: computed tomographic and neuropathologic correlation. *Radiology* 1979;133:113–122
63. Enzmann DR, Britt RH, Placone R. Staging of human brain abscess by computed tomography. *Radiology* 1983;146:703–708
64. Haimes AB, Zimmerman RD, Morgello S, et al. MR imaging of brain abscess. *AJNR* 1989;10:279–291
65. Brook I. Bacteriology of intracranial abscess in children. *J Neurosurg* 1981;54:484–488
66. Berthier M, Sierra J, Leiguarda R. Intraventricular tuberculoma. *Neuroradiology* 1987;29:163–167
67. Schoeman JF, Hewlett R, Donald P. MR of childhood tuberculous meningitis. *Neuroradiology* 1988;30:473–477
68. Chang H, Han MH, Roh JK, et al. Gd-DTPA enhanced MR imaging in intracranial tuberculosis. *Neuroradiology* 1990;32:19–25
69. van Dyk A. CT of intracranial tuberculomas with specific reference to the "target sign." *Neuroradiology* 1988;30:329–336
70. Weinberg S, Bennett H, Weinstock I. Central nervous system manifestations of sarcoidosis in children. *Clin Pediatr* 1983;22:477–481
71. Hayes WS, Sherman JL, Stern BJ, Citrin CM, Pulaski PD. MR and CT evaluation of intracranial sarcoidosis. *AJNR* 1987;8:841–847
72. Fernandez RE, Rothberg M, Ferencz G, Wujack D. Lyme disease of the CNS: MR imaging findings in 14 cases. *AJNR* 1990;11:479–481
73. Rafto SE, Milton WJ, Galetta SL, Grossman RI. Biopsy-confirmed CNS lyme disease: MR appearance at 1.5T. *AJNR* 1990;11: 482–484
74. Byrd SE, Locke GE, Biggers S, Percy AK. The computed tomographic appearance of cerebral cytsticercosis in adults and children. *Radiology* 1982;144:819–823
75. Kramer LD, Locke GE, Byrd SE, Daryabagi J. Cerebral cysticercosis: documented of natural history with CT. *Radiology* 1989;171: 459–462
76. Martinez HR, Rangel-Guerra R, Elizonda G, Gonzalez J, et al. MR imaging in neurocysticercosis: a study of 56 cases. *AJNR* 1989;10: 1011–1019
77. Lotz J, Hewlett R, Alheit B, Bowen R. Neurocyticercosis: correlative pathomorphology and MR imaging. *Neuroradiology* 1988;30:35–41
78. Suss RA, Maravilla KR, Thompson J. MR imaging of intracranial cysticercosis: comparison with CT and anatomopathologic features. *AJNR* 1986;7:235–242